Protein J
DOI 10.1007/s10930-017-9744-8

High Yield Preparation of Functionally Active Catalytic-Translocation Domain Module of Botulinum Neurotoxin Type A That Exhibits Uniquely Different Enzyme Kinetics

Harkiranpreet Kaur Dhaliwal[1,5] · Nagarajan Thiruvanakarasu[2,4] · Raj Kumar[3] · Kruti Patel[2] · Ghuncha Ambrin[1] · Shouwei Cai[2] · Bal Ram Singh[3]

Abstract Botulinum neurotoxins (BoNTs) are the most toxic proteins known to cause flaccid muscle paralysis as a result of inhibition of neurotransmitter release from peripheral cholinergic synapses. BoNT type A (BoNT/A) is a 150 kDa protein consisting of two major subunits: light chain (LC) and heavy chain (HC). The LC is required for the catalytic activity of neurotoxin, whereas the C and N terminal domains of the HC are required for cell binding, and translocation of LC across the endosome membranes, respectively. To better understand the structural and functional aspects of BoNT/A intoxication we report here the development of high yield *Escherichia coli* expression system (2–20-fold higher yield than the value reported in the literature) for the production of recombinant light chain-translocation domain (rLC-TD/A) module of BoNT/A which is catalytically active and translocation competent. The open reading frame of rLC-TD/A was PCR amplified from deactivated recombinant BoNT/A gene (a non-select agent reagent), and was cloned using pET45b (+) vector to express in *E. coli* cells. The purification procedure included a sequential order of affinity chromatography, trypsinization, and anion exchange column chromatography. We were able to purify > 95% pure, catalytically active and structurally well-folded protein. Comparison of enzyme kinetics of purified LC-TD/A to full-length toxin and recombinant light chain A suggest that the affinity for the substrate is in between endopeptidase domain and botulinum toxin. The potential application of the purified protein has been discussed in toxicity and translocation assays.

Keywords Botulinum neurotoxin type A · Recombinant light chain-translocation domain rLC-TD/A · Protein purification · Site-directed mutagenesis · Potassium channel assay · Enzyme kinetics · Translocation · SNAPtide® activity · Cell-based SNAP-25 assay

Abbreviations

BoNT	Botulinum neurotoxin
BoNT/A	Botulinum neurotoxin Type A
DTT	Dithiothreitol
DNA	Deoxyribonucleic acid
DrBoNT/A	Deactivated botulinum neurotoxin type A
E.coli	*Escherichia coli*
EDTA	Ethylenediaminetetraacetic acid
FRET	Fluorescence resonance energy transfer
GST	Glutathione-S-transferase
HC	Heavy chain
IPTG	Isopropyl-b-D-thiogalactopyranoside
LB	Luria–Bertani
LC	Light chain
PCR	Polymerase chain reaction
RBD	Receptor binding domain
rLC-TD/A	Recombinant light chain-translocation domain

✉ Bal Ram Singh
bsingh@inads.org

[1] Biomedical Engineering and Biotechnology Program, University of Massachusetts Dartmouth, North Dartmouth, MA 02747, USA

[2] Department of Chemistry and Biochemistry, University of Massachusetts Dartmouth, North Dartmouth, MA 02747, USA

[3] Botulinum Research Center, Institute of Advanced Sciences, Dartmouth, MA 02747, USA

[4] Present Address: US Food and Drug Administration, Silver Spring, MD, USA

[5] Present Address: Department of Pharmaceutical Sciences, Northeastern University, Boston 02115, USA

Published online: 13 October 2017

SDS-PAGE	Sodium dodecyl sulfate-polyacrylamide gel electrophoresis
SNAP-25	Synaptosome associated protein of 25 kDa
SNARE	Soluble *N*-ethylmaleimide-sensitive factor attachment protein
TD	Translocation domain

1 Introduction

The Clostridial neurotoxin family constitutes *Clostridia tetani*, which produces tetanus neurotoxin and *Clostridium botulinum* which produces seven (A–G) antigenically different types of botulinum neurotoxin (BoNT). BoNTs are zinc dependent endopeptidases known to cause flaccid paralysis as a result of blockage of neurotransmission at the synapse region of peripheral neurons by cleaving soluble *N*-ethylmaleimide-sensitive factor attachment protein receptor (SNARE) which is involved in the vesicle fusion and docking at the neuronal membrane [1]. The cleavage of the SNARE protein is very specific and serotype dependent which contributes to the immense toxicity and potency of BoNT molecule.

BoNTs are 150 kDa di-chain neurotoxins produced as a single chain polypeptide by *Clostridium* genus bacteria in its cytosol without a leader sequence [2]. The single chains are biologically inactive which upon nicking by endogenous or exogenous proteases turn into highly toxic di-chains composed of 100 kDa heavy chain (HC), and 50 kDa light chain (LC), connected covalently via a single interchain disulfide bond [3, 4]. The HC can be divided into two domains: the N-terminal (translocation domain, TD; 50 kDa) and C-terminal domain (receptor-binding domain, RBD; 50 kDa) [5]. The TD inserts into the endosomal membrane at low pH and forms transmembrane ion channels [4–7] and RBD assists in neuro-specific binding [8]. Among the seven serotypes, BoNT type A (BoNT/A) is the most toxic as well as widely used clinical serotype [9]. Recent findings indicate BoNT/A TD's role not only as a channel forming domain but also as a chaperone for the transmembrane translocation of LC in the neuronal cells [10–13]. The LC domain of BoNT/A specifically cleaves t-SNARE, synaptosome associated protein of 25 kDa (SNAP-25), resulting in the inhibition of neurotransmission at the synapse of peripheral neurons.

The BoNT/A structure constitutes trypsin nicking sites which can be utilized to derive the LC-TD/A region that can be purified from the toxin preparations [14]. Other methods of non-clostridial source rLC-TD/A expression in *Escherichia coli* includes either amplification of LC-TD/A region from BoNT/A gene sequence produced with glutathione-S-transferase (GST) tag [15] or ligation of LC and TD gene sequences from separate vectors [13, 16]. However, the yield reported has been extremely low (~0.073 mg per g cell paste with 88.5% purity [15] and 0.8 mg per g cell paste with > 95% purity [16]). In the present work, we have developed an improved method of rLC-TD/A expression system which produced better yield (1.50 mg per g cell paste) and purity (> 95%) of protein than reported by earlier published methods. In addition to the improved purification process, we have also shown the potential use of rLC-TD/A protein in in vitro SNAPtide® activity assay, cell based SNAP-25 assay and liposome driven translocation assay. Hence, the rLC-TD/A protein purified by our method could be exploited in the translocation mechanism studies, toxicity assays, and in drug delivery methodologies.

2 Materials and Methods

The oligonucleotides were synthesized by Integrated DNA Technologies (Coralville, IA). In-Fusion® HD Cloning kit from Clontech Laboratories, Inc (Mountain View, CA) and QuikChange Lightning Multi Site-Directed Mutagenesis kit (including *E. coli* XL-1 Blue competent cells) was from Agilent Technologies Inc (Lexington, MA). E. cloni® 10G chemically competent cells for cloning process and *E.coli* BL21-CodonPlus (DE3)-RIL cells for protein over expression were from obtained from Lucigen Corp (Middleton, WI). The QIAquick Gel extraction kit was purchased from Qiagen, plasmid pET-45b (+) from Novagen (Madison, WI), genomic deoxyribonucleic acid (DNA) isolation kit from Promega (Madison, WI), and restriction endonucleases were obtained from New England BioLabs (Beverly, MA). Thermal cycler used for polymerase chain reaction (PCR) was from Eppendorf-Netheler-Hinz GmbH (Hamburg, Germany). Deoxyribonucleotide (DNA) sequencing was confirmed by Genewiz DNA sequencing (Cambridge, MA). HisPur™ Cobalt resin was obtained from Thermo Fisher Scientific Corp (USA). Isopropyl-b-D-thiogalactopyranoside (IPTG) was obtained from RPI Corp (Mt Prospect, IL) and SNAPtide®520 (oAbz/Dnp) and SNAPtide®521 (FITC/DABCYL) peptide substrate for *Clostridium botulinum* Type A neurotoxin was from List Biological Laboratories Inc (Campbell, CA, U.S. Patent #6,504,006). All chemicals were purchased from Sigma Aldrich (St. Louis, MO) unless otherwise specified.

2.1 Primer Design and Amplification of rLC-TD/A

The DNA fragment for rLC-TD/A was obtained from deactivated recombinant BoNT/A (DrBoNT/A) vector clone [17] that is exempted by CDC from the select agent regulations. DrBoNT/A clone produces catalytically inactive protein consisting of two glutamic acid mutations (E224 and E262) to alanine at the active site of BoNT/A LC which has been demonstrated by in vitro SNAPtide® [17] and mouse

neuromuscular junction assay [18]. Primers were designed for the amplification of rLC-TD/A region from DrBoNT/A according to the BoNT/A sequence in the GenBank database under Accession No. Q7B8V4 (Fig. 1). PCR reaction for the amplification of rLC-TD/A DNA fragment included: 1X PCR buffer (10 mM Tris–HCl, pH 8.3, 1.5 mM $MgSO_4$, 50 mM KCl and 0.1% Triton X-100), 100 ng of template DNA, 100 ng of each primer, 0.2 mM of dNTPs (deoxynucleoside triphosphate), and 1.25 U *Taq* polymerase, made up to a total volume of 50 µl with RNAse free water. The PCR reaction was carried out in a programmable thermocycler using following parameters: initial denaturation at 95 °C for 3 min; followed by two consecutive cycles consisting of denaturation at 95 °C for 30 s, annealing for 1 min at 46 °C, and extension at 68 °C for 3 min; 32 cycles consisting of denaturation at 95 °C for 30 s, annealing for 45 s at 57 °C, and extension at 68 °C for 3 min; and final extension cycle of 5 min at 68 °C. The PCR amplified rLC-TD/A DNA fragment was produced with *Pml*I and *Xho*I restriction sites at the 5′ and 3′ ends, respectively.

2.2 Gene Construction of rLC-TD/A Clones

The rLC-TD/A PCR amplified product was treated with Taq polymerase at 72 °C for 10 min, required for addition of adenine on each end of the rLC-TD/A DNA fragment. The rLC-TD/A DNA fragment was eluted using the QIAquick gel extraction kit. The rLC-TD/A DNA fragment purified from agarose gel electrophoresis was cloned into *Pml*I/*Xho*I digested pET45b (+) vector using Clontech In-Fusion® HD cloning kit and E. cloni® 10G chemically competent cells. The rLC-TD/A DNA fragment was cloned with the His6-tag at the N-terminal end. The colonies grown on Luria–Bertani (LB) ampicillin agar plates were used for recombinant plasmid extraction. The clones were then digested using *Pml*I and *Xho*I restriction enzymes and the open reading frame confirmation was carried out using DNA sequencing (dideoxy chain termination method) on the selected plasmids of expected size. The presence of a correct gene sequence of the rLC-TD/A plasmid (encoding 871 amino acids corresponding to LC-TD/A sequence) was confirmed by comparing the sequence with BoNT/A sequence in the GenBank database using Expert Protein Analysis System (ExPASy) Molecular Biology Server.

2.3 Site-directed Mutagenesis for Production of Catalytically Active rLC-TD/A

Site-directed mutagenesis of the LC region was carried out using the QuikChange Lightning Multi Site-Directed Mutagenesis kit to produce catalytically active rLC-TD/A plasmid. The alanine 224 and 262 residues were mutated into glutamic acid residues using the primers designed as shown in Fig. 2. pET45b (+) ligated rLC-TD/A plasmid was used as a template in the mutagenesis reaction. The site directed mutagenesis reaction included: 100 ng of chromosomal DNA as template DNA, 125 ng of each primer, 5.0 µl of 10× reaction buffer, 1.0 µl concentration of dNTP (deoxy nucleoside triphosphate), 1.5 µl of Quick solution reagent and 1.0 µl QuickChange Lightning enzyme made up to a

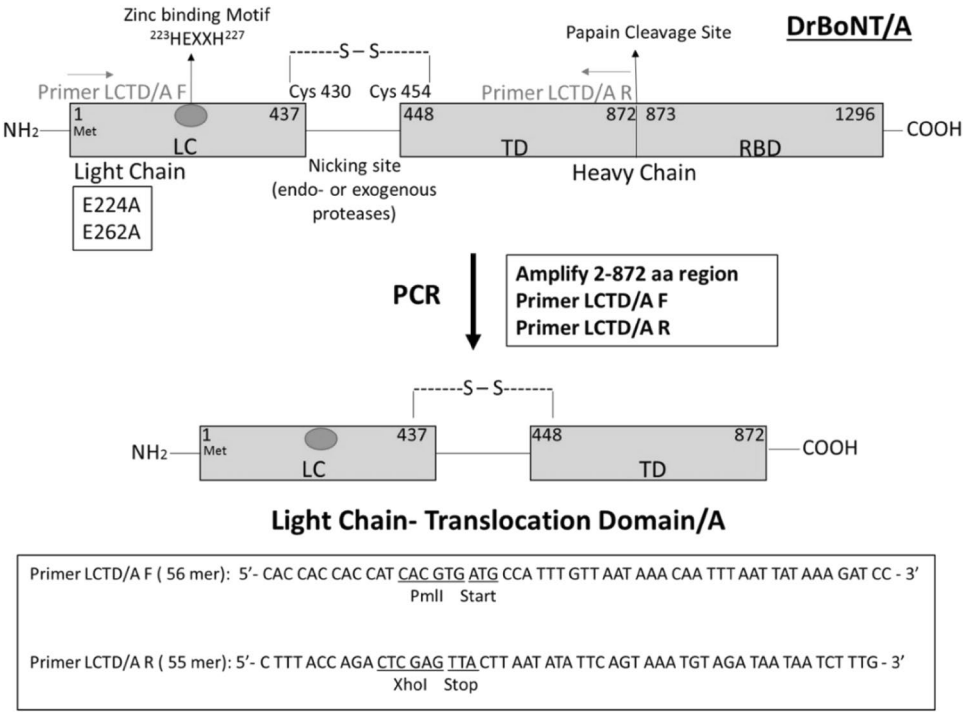

Fig. 1 Structure model of DrBoNT/A, and primers utilized in the PCR amplification of the LC-TD/A region. LC represents light chain, TD represents translocation domain and RBD represents receptor binding domain of DrBoNT/A. The forward and reverse primers used for LC-TD/A amplification are designated as Primer LCTD/A F and Primer LCTD/A R, respectively. The sequences corresponding to both primers are highlighted in a rectangular box with underlined restriction sites for *Pml*I and *Xho*I restriction enzymes

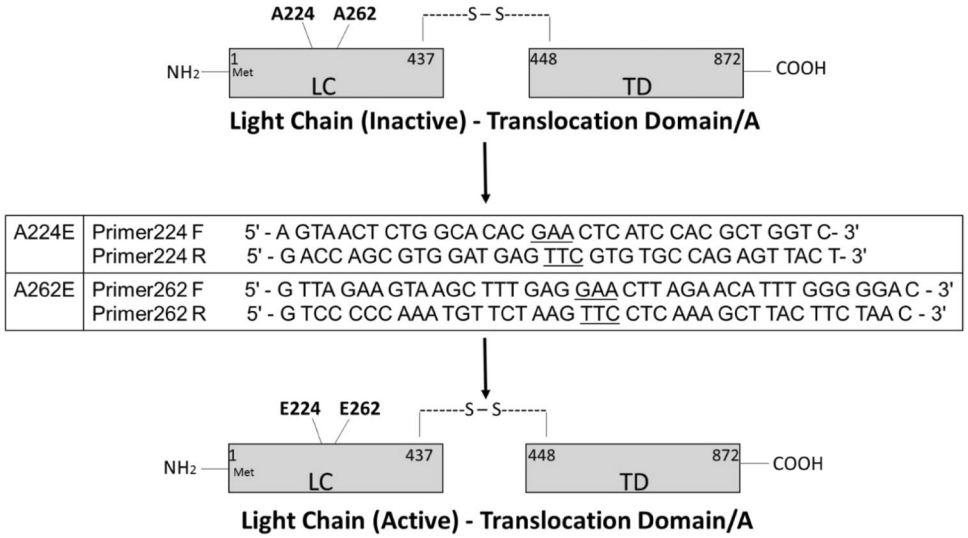

Fig. 2 Schematic representation of site-directed mutagenesis to produce catalytically active rLC-TD/A. The alanine (A) 224 and 262 residues are mutated into glutamic acid (E) residues to activate the substrate binding region of rLC-TD/A. The primers utilized in the mutagenesis process are highlighted in a rectangular box. F represents forward primer and R represents a reverse primer for the respective mutation sites. The mutated nucleotide bases are underlined in the primer sequences

total volume of 50 µl with RNAse free water. PCR reaction for mutagenesis reaction was performed using the following conditions: initial denaturation for 2 min at 95 °C; 30 cycles of 20 s at 95 °C (denaturation), 30 s at 55 °C (annealing) and 4 min at 65 °C (extension, 30 s/kb) and final extension for 5 min at 65 °C. The amplified PCR product was kept at 4 °C for 5 min, and was subsequently digested using Dpnl for 10 min at 37 °C. The amplified plasmid was then transformed into *E. coli* XL-1 Blue competent cells. The colonies grown on LB ampicillin agar plates were screened for correct plasmid constructs by performing digests with *Pml*I and *Xho*I enzymes and running samples on 1% agarose gels [19]. The presence of the enzymatically active rLC-TD/A plasmid was confirmed by DNA sequencing and by comparing its sequence with the BoNT/A sequence in the GenBank database. The catalytically active rLC-TD/A plasmid was designated as pET45b (+)-rLCTD/A.

2.4 Expression and Purification of rLC-TD/A

The pET45b (+)-rLCTD/A plasmid was transformed into *E. coli* BL21-CodonPlus (DE3)-RIL cells for the expression of N-terminal His-tagged rLC-TD/A protein under the control of T7 promoter, as per the manufacturer's instructions. For expression of rLC-TD/A protein, *E. coli* cells were plated on LB ampicillin agar plates. Several single colonies were cultured in 2YT medium (5 ml) (1.6% tryptone, 1% yeast extract, and 0.5% NaCl) and were induced using IPTG to test for the highest expression of rLC-TD/A. The samples were tested for the expression of the protein on a 12% sodium dodecyl sulfate-polyacrylamide gel electrophoresis (SDS-PAGE) [20]. The highest expressing colony culture was used to inoculate 10 ml of 2YT medium supplemented with 100 µg/ml ampicillin. The culture was grown overnight at 37 °C. The 10 ml aliquot was then used to inoculate 1 l of 2YT medium in a 4-l Pyrex flask, and the culture was grown at 37 °C to 0.6 OD_{600}. The protein expression was carried out at a lower temperature of 18 °C using IPTG induction at a final concentration of 1 mM. The cells were harvested after 16 h of IPTG induction, and were pelleted down by centrifugation at 5000×*g* for 10 min at 4 °C. The cell pellets were stored at − 80 °C until the protein purification was carried out.

The frozen pellets were thawed and were re-suspended in the lysis buffer (20 mM Tris–HCl buffer, pH 7.8, containing 300 mM NaCl, 5 mg/ml lysozyme, and ethylenediaminetetraacetic acid (EDTA)-free protease inhibitor cocktail). The cell lysis was carried out at 4 °C for 20 min. Next, sonication was performed on the suspended cells to disrupt the cells by three alternate cycles of sonication and ice incubation. Sonication was performed for 30 s with 1 s on and off procedure at 12 W output. 5 µg/ml deoxyribonuclease-I was added after sonication to digest DNA in the sample which leads to the reduction in viscosity of the samples. The resulting cell lysate was centrifuged at 11,000×*g* for 30 min at 4 °C to separate the proteins into soluble and insoluble fractions. The rLC-TD/A was purified using three sequential steps: cobalt affinity column chromatography, followed by trypsinization, and anion exchange column. All the steps of purification process were carried out at 4 °C unless otherwise specified. The supernatant obtained after removing insoluble fraction was loaded onto cobalt column pre-equilibrated with equilibration buffer (20 mM Tris–HCl, pH 7.8, containing 300 mM NaCl). The column was sequentially washed with equilibration and wash buffer (equilibration buffer containing 5 mM imidazole). The protein was eluted with 200 mM imidazole in an equilibration buffer till the 280 nm reading reached baseline levels. The pooled fractions of protein were dialyzed overnight with the equilibration buffer.

Dialyzed protein was trypsinized in a 200:1 (protein: trypsin, w/w) ratio for 90 min at 25 °C. The resulting protein solution was incubated with trypsin agarose beads (2 mg/ml binding capacity for trypsin) at 25 °C for 20 min on a rotor to remove trypsin.

The pI of rLC-TD/A was calculated to be ~5.85 using online software (http://isoelectric.ovh.org/). Therefore, anion-exchange (QAE Sephadex A-50, GE Healthcare Life Sciences) column chromatography was selected as the next step in purification. The supernatant was dialyzed after removal of trypsin in a stepwise gradient of NaCl against 20 mM Tris–HCl buffer, pH 6.5, containing 300, 200, 100 and 20 mM NaCl. 20 mM NaCl was kept in the buffer to reduce the precipitation of protein. The dialyzed protein solution was loaded onto QAE A-50 column pre-equilibrated with buffer (20 mM Tris–HCl, pH 6.5, containing 20 mM NaCl). The protein was eluted with increasing concentration of NaCl. The fractions obtained at each step of purification were tested on SDS-PAGE for purity. For further studies, the rLC-TD/A protein was stored in the buffer (20 mM Tris–HCl, pH 7.4, containing 300 mM NaCl) containing 20% glycerol solution at − 80 °C after flash freezing.

2.5 Protein Concentration Estimation

The protein concentration was measured using the Pierce protein assay method (Thermo Fisher Scientific, PA). A standard curve was obtained using Bovine Serum Albumin (Biorad Laboratories, CA) and a linear regression method was used for the measurement of protein concentration.

2.6 SDS-PAGE and Western Blotting

SDS-PAGE [20] and Western blotting [21] were performed for the estimation of protein purity using standard protocols. Briefly, 12% SDS-PAGE was used for protein separation based on molecular size and the proteins were transferred to nitrocellulose membranes for western blotting. The binding of primary antibody anti-BoNT/A raised in rabbit (Prime Bio Inc., Dartmouth, MA) was visualized using alkaline phosphatase conjugated secondary antibody goat anti-rabbit (Sigma Aldrich) and a colorimetric alkaline phosphatase detection system (BCIP/NBT substrate) (Bio-Rad Laboratories, CA). The gels and blots were scanned on a Gel Logic 100 Imager system (Cole-Parmer). The gels stained using Coomassie blue stain were assessed for density estimation using GelQuant.NET software provided by biochemlabsolutions.com. To estimate the purity of protein, the protein of interest band was compared with the rest of the bands in the respective lanes.

2.7 In Vitro SNAPtide® Peptide Assay

The endopeptidase activity and enzyme kinetic were assessed using SNAPtide® 521 peptide substrate which utilizes 17-mer FRET peptide containing a cleavage site segment of SNAP-25. The protocol was followed according to the manufacturer's instructions. The assay was performed in a 96 well plate format (Costar® 96- Well Black Polystyrene Plate). Briefly, for activity assay, 100 nM rLC-TD/A was pre-incubated in a total volume of 100 µl reaction buffer (20 mM Hepes pH 7.4 containing 1.25 mM dithiothreitol (DTT) and 0.1% TWEEN-20) for 20 min at 37 °C. 2.5 µM SNAPtide® 521 was added to the wells and fluorescence reads were taken at various time points using SpectraMax M5 microplate reader (Molecular Devices, Menlo Park, CA, USA).

The enzyme kinetics was performed at 37 °C for the first ten minutes using 50 nM rLC-TD/A and various concentrations (0–8 µM) of SNAPtide® 521 and the kinetic parameters were calculated according to the published protocol [22]. The hydrolysis of the substrate was monitored with 490 nm excitation and 523 nm emission. Excitation and emission slit widths were fixed at 4 nm. The final measurement was done after subtracting blank readings (reaction buffer and SNAPtide®). The increase in fluorescence signal, with respect to blank, indicates the extent of cleavage of the substrate or increase in activity of the protein. The RFU values were converted into µM using the method described in the published work [22]. Kinetic parameters were determined using the Lineweaver–Burk plot.

The enzyme kinetics of BoNT/A was carried out using different concentrations of SNAPtide® 520 ranging between 10 to 100 µM (10, 12.5, 15, 25, 50, and 100). The reaction was determined for the first 5 min at 37 °C. BoNT/A toxin was dissolved in 20 mM HEPES buffer [0.3 mM $ZnCl_2$, 1.25 mM DTT and 0.1% of Tween 20 (pH 8.0)] to a final concentration of 100 nM and was incubated at 37 °C for 30 min before adding it to the reaction mixture (750 µl). The Excitation wavelength was 320 nm and the emission spectra were recorded between 340 and 460 nm, using the ISS K2 spectrophotometer (ISS Inc., Urbana, IL). The excitation and emission slit widths were fixed at 16 and 4 nm respectively.

2.8 Cell-based SNAP-25 Activity Assay

For cell-based SNAP-25 activity assay, cell lysates were tested for activity of rLC-TD/A by conducting an immunoblot for detection of cleaved SNAP-25 as described with modifications [23]. Briefly, the SH-SY5Y neuroblastoma cells (ATCC, Manassas, VA) were routinely grown and passaged in 25 cm^2 culture flasks. The cells were maintained in a 37 °C/5% CO_2 humidified incubator in MEM growth medium containing 10% FBS (Sigma

Aldrich, St. Louis, MO). For activity assay, the SH-SY5Y neuroblastoma cells were seeded at a density of 120,000 cells per well in a 12-well tissue culture plate. After 24 h of growth, cells were incubated with 50 nM rLC-TD/A or BoNT/A for the next 48 h. The cells were washed with cold phosphate buffer saline solution and were harvested using M-PER reagent (Thermo Fisher Scientific, PA) which dissolves the membrane proteins, after the completion of the reaction. Samples were run on a 15% SDS-PAGE. The protein bands were electro-transferred onto nitrocellulose membrane and Western blot analysis was performed for SNAP-25 bands using a primary antibody (anti-SNAP-25 monoclonal antibody raised in rabbit, Sigma Aldrich) and an alkaline phosphate conjugated secondary antibody (goat anti-rabbit alkaline phosphate conjugate, Sigma Aldrich). The final visualization was carried out by using alkaline phosphatase substrate NBT/BCIP (Sigma Aldrich). The intensity of the cleaved band at 24 kDa was compared with the un-cleaved 25 kDa, SNAP-25 band, to observe the % activity of BoNT or rLC-TD/A inside the neuronal cells.

2.9 Potassium Ion Release Assay for Membrane Channel Formation

The potassium ion (K^+) release assay was performed as described with modifications [24]. Briefly, the liposomes were prepared by thin film hydration approach [25], using 12.5 mg/ml of asolectin and cholesterol lipids (Sigma Aldrich Inc., St. Louis, MO) in a 2:1 mol ratio in chloroform. The residual traces of organic solvent were removed by vacuum drying for 2 h. The vesicles were rehydrated using potassium rehydration buffer: 100 mM potassium phosphate buffer pH 7.2, containing 1.5 mM EDTA. For the K^+ release assay, K^+ loaded pH 7.2 liposomes were incubated with 100 nM of rLC-TD/A protein in 100 mM citrate/phosphate buffer, pH 4.5, containing 100 mM NaCl and 1.5 mM EDTA. The K^+ release measurements for rLC-TD/A were carried out with increase in time in a *trans*-compartmental system at 25 °C (signal was recorded in a continuous mode), with the K^+ selective electrode (Orion Star, Thermo Scientific, Pittsburgh, PA) connected to a microcomputer pH/mV/Temp meter 6171. The basal release was subtracted from the individual reads and the total K^+ release was estimated by adding 0.5% octylglucoside detergent (Sigma Aldrich., St. Louis, MO) after the end point measurement. The control with only buffer, channel-forming peptide Gramicidin A (positive control), and trypsin (negative control) was included in the experiments for comparison of results between two different liposome preparations.

2.10 Circular Dichroism Spectroscopy

CD data was collected using JASCO J-715 spectropolarimeter (Jasco Inc., Easton NJ) equipped with a Peltier temperature control (Model PTC-348 W) as described previously [26]. The protein was dialyzed in 20 mM Tris–HCl pH 7.4 buffer, containing 300 mM NaCl for CD spectra measurements. Far-UV CD spectra was recorded in the 190–250 nm wavelength region in a 1.0 mm path length cuvette with a protein concentration of 0.2 mg/ml at 25 °C at a scanning speed of 20 nm/min and with a response time of 8 s. A total of three scans were recorded and averaged to increase the signal to noise ratio. The final spectra were obtained after correcting the buffer contribution. The data presented was normalized for the concentration of protein, path length and was expressed as Mean Residue Ellipticity (degree cm^2/dmol). The secondary structure content was estimated using K2D3 software [27].

3 Results

3.1 Construction of pET45b (+)-rLCTD/A Plasmid

The pET45b (+)-rLC-TD/A plasmid with active LC region produced by PCR amplification and cloning was tested using single and double digestion using restriction enzyme reaction. The single digestions with *Xho*I and *Pml*I separately showed 7.8 kb fragment band corresponding to the linearized pET45b (+)-rLCTD/A, and double digestion with *Xho*I + *Pml*I showed 5.15 and 2.65 kb band corresponding to pET45b (+) vector and rLC-TD/A, respectively (Fig. 3). DNA sequencing and amino acid sequencing confirmed the presence of DNA fragment encoding 871 amino acids corresponding to LC-TD/A sequence.

3.2 Expression and Purification of His-tagged rLC-TD/A

IPTG was used to express His6-tagged rLC-TD/A at a reduced temperature of 18 °C which facilitates high yield of protein by reducing its degradation, and decreasing the expression of *E. coli* proteins. The supernatant collected after pelleting down of insoluble material of lysed cells showed the presence of ~101 kDa band corresponding to the rLC-TD/A which confirmed the expression of the protein from the clone developed (Fig. 4). The flow through (FT) of cobalt column did not show any significant loss of protein at least to the limits of SDS-PAGE, indicating binding of rLC-TD/A to the column under the conditions mentioned. Equilibration buffer with 5 mM imidazole lead to significant elution of rLC-TD/A protein. The rest of the protein was eluted using 200 mM imidazole in equilibration buffer. The

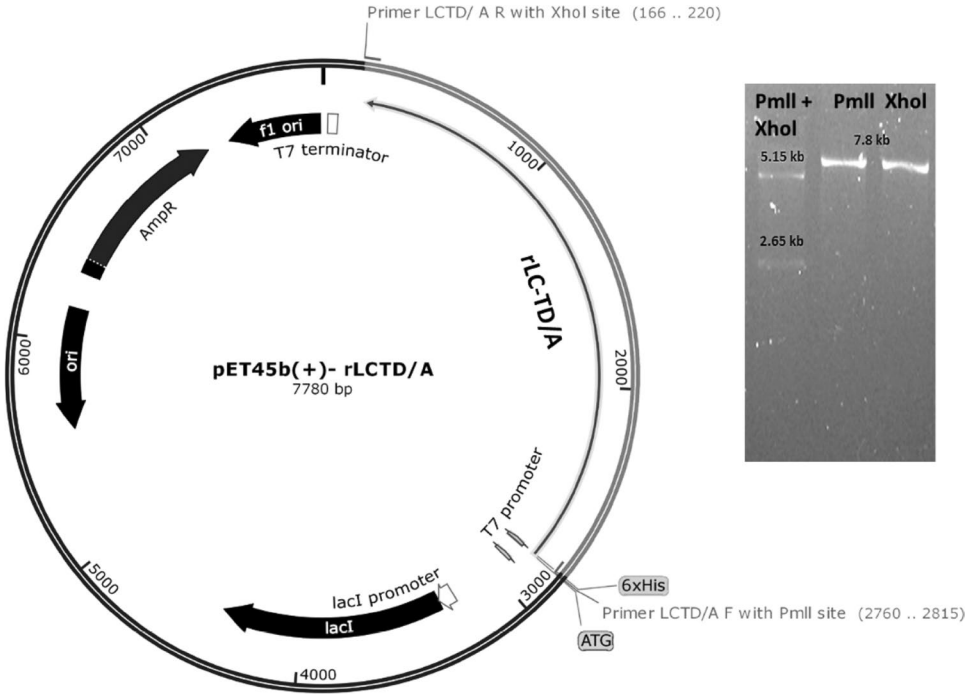

Fig. 3 Construction of the recombinant vector pET45b (+) containing the cassette for rLC-TD/A expression using SnapGene® software. The forward (Primer LCTD/A F) and reverse (Primer LCTD/A R) primers were designed, containing *Pml*I and *Xho*I restriction sites, respectively. The inset figure shows the agarose gel electrophoresis of *Pml*I + *Xho*I digested recombinant vector, where 5.15 kb excised fragment represents linearized pET45b (+) vector fragment and 2.65 kb fragment represents rLC-TD/A fragment. The single digestion reaction using *Pml*I or *Xho*I shows a ~7.8 kb fragment corresponding to linearized pET45b (+)-rLCTD/A plasmid

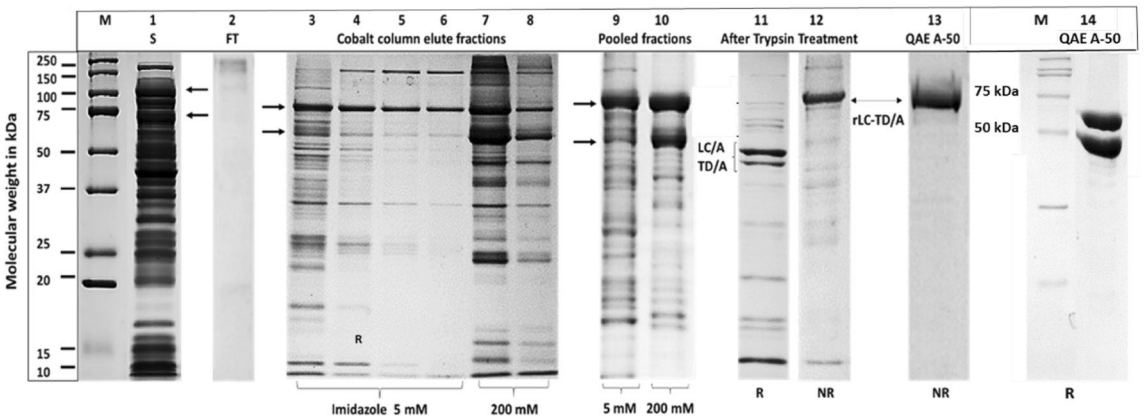

Fig. 4 SDS-PAGE analysis for purification steps of rLC-TD/A protein. M represents precision plus protein™ Kaleidoscope™ standards (Biorad), the numbers on the left indicate molecular weight of standards in kDa, lane 1: supernatant of cell lysate after removal of insoluble protein (S), lane 2: flow through fraction of supernatant after protein binding to cobalt column (FT), lane 3–6: 5 mM imidazole elute fraction, lane 7–8: 200 mM imidazole elute fraction, lane 9: 5 mM imidazole pooled fraction after dialysis, lane 10: 200 mM imidazole pooled fraction after dialysis, lane 11: trypsinized and DTT reduced affinity pooled fraction (R), lane 12: trypsinized and non-reduced affinity pooled fraction (NR), lane 13: non-reduced fraction of QAE-A50 eluted rLC-TD/A, lane 14: reduced fraction of QAE-A50 eluted rLC-TD/A. 200 mM imidazole elute fraction showed ~101 kDa rLC-TD/A protein band and a major impure band at ~74 kDa as indicated by arrows. Trypsinization step lead to digestion of ~74 kDa impure band (lane 11 & 12). Reduction of QAE A-50 column eluted fractions shows protein bands at ~52, and ~49 kDa, corresponding to LC/A and TD/A, respectively (lane 14)

200 mM imidazole elute fractions showed more impurities as compared to the fractions collected using 5 mM imidazole. The results showed co-elution of a major impurity band at ~74 kDa along with rLC-TD/A ~101 kDa band in 200 mM imidazole fractions (Fig. 4). Trypsinization, after affinity chromatography, was performed for nicking of rLC-TD/A, which also resulted in the digestion of other impurities, majorly 74 kDa. Nicking efficiency was confirmed by the presence of bands at ~52.2 and ~48.8 kDa corresponding to His6-tag LC/A and TD/A, respectively (Fig. 4).

The pure rLC-TD/A protein was eluted between 50 and 70 mM NaCl salt gradient in anion-exchange column. (QAE-A50 column). The purity of the eluted protein was determined to be > 95% as assessed by the SDS-PAGE with

a yield of 1.50 ± 0.35 mg protein per g cell paste. Table 1 shows the percentage purity of rLC-TD/A at each step of purification as measured from the coomassie blue stained gels. The western blot analysis of final rLC-TD/A fraction run under reducing conditions confirmed the identity of rLC-TD/A by displaying two protein bands corresponding to LC/A and TD/A at ~52.2, and ~48.8 kDa, respectively (Fig. 5).

3.3 Endopeptidase Assay

The enzymatic activity of rLC-TD/A protein was assessed using in vitro SNAPtide® 521 peptide assay and cell-based SNAP-25 cleavage assay. rLC-TD/A showed 1451.3 ± 117.8, 3565.0 ± 145.5, 5211 ± 109.1 and 7254.8 ± 101.1 relative fluorescence units (RFU) after 5, 10, 15, and 20 min of substrate addition to the reaction, respectively (Fig. 6a). The increase in RFU value with increase of time indicated that the purified rLC-TD/A is active. Kinetic parameters were calculated from the regression equation obtained from the Lineweaver–Burk plot for rLC-TD/A (Fig. 7). The K_m was calculated to be 30.8 ± 8.4 µM, K_{cat}: 0.052 ± 0.010 s^{-1}, and K_{cat}/K_m: 0.0016 ± 0.0006 s^{-1} M^{-1}. The corresponding values for intact BoNT/A (reduced) using SNAPtide® 520 as substrate was K_m: 100.58 ± 9.20 µM, K_{cat}: 0.343 ± 0.018 s^{-1}, and K_{cat}/K_m: 0.0033 ± 0.0001 s^{-1} M^{-1}, respectively.

The cell based endogenous SNAP-25 cleavage assay is widely used as an activity test for BoNT in the neuronal cell culture. The addition of 50 nM rLC-TD/A and BoNT/A for 48 h resulted in 44.20 ± 3.67 and 60.0 ± 2.3% cleavage of SNAP-25, respectively (Fig. 6b). The cells pretreated with 2 µM bafilomycin and subsequently with rLC-TD/A did not show SNAP-25 substrate cleavage.

3.4 Channel Formation by rLC-TD/A in Liposomes

The K^+ release from asolectin vesicles has been widely used as a method to detect low pH induced channel formation by BoNT and its subunits [7]. The addition of Gramicidin A to the liposomes at pH 7.2 and 4.5 showed 30.28 ± 0.80 and 32.13 ± 0.60% release of K^+, respectively, at 5 min time point (Fig. 8). The similar amount of K^+ release from vesicles at pH 7.2 and pH 4.5 indicates that the vesicles are not damaged by their transfer from

Table 1 Purification table for rLC-TD/A

Purification stage	Clarified cell lysate extract	Cobalt-affinity 5 mM imidazole	Cobalt-affinity 200 mM imidazole	Post-dialysis and trypsin treatment	QAE A-50 fraction
Volume	70.0	22.0	15.0	39.0	14.0
Total protein[a] (mg) (n = 6)	NA	34.0 ± 4.7	20.8 ± 4.0	23.0 ± 3.5	10.5 ± 2.5
rLC-TD/A % purity[b] (n = 6)	7.5 ± 1.8	42.5 ± 6.2	22.6 ± 4.5	48.3 ± 3.5	> 95%
Yield (mg rLC-TD/A per g cell paste) = 1.50 ± 0.35 (n = 6)					

[a]Denotes the total protein calculated using pierce 660 nm protein assay

[b]Denotes the percentage of rLC-TD/A protein calculated from coomassie blue stained gels. NA denotes not assessed. The purity of protein was assessed by densitometry scanning of coomassie blue stained SDS-PAGE gels using GelQuant.NET software. The data presented here is of six independent experiments and is mean ± standard deviation

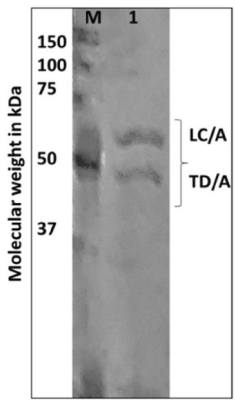

Fig. 5 Western blot analysis of nicked and reduced rLC-TD/A protein. M represents precision plus protein™ Kaleidoscope™ standards (Biorad) in kDa. Lane 1 represents QAE A-50 eluted reduced and nicked rLC-TD/A fraction. Anti-BoNT/A antibody detected two bands at ~52 and ~49 kDa corresponding to rLC/A and TD/A, respectively confirming the identity of protein. The visualization of protein bands was carried out by using alkaline phosphatase substrate NBT/BCIP colorimetric assay

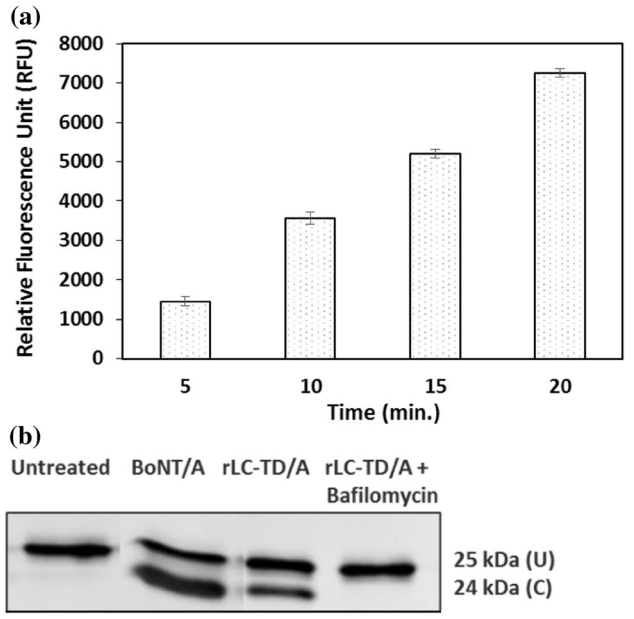

Fig. 6 The endopeptidase activity estimate for rLC-TD/A using **a** in vitro SNAPtide® and **b** cell based SNAP-25 cleavage assay. The SNAPtide® peptide assay conducted at 37 °C showed an increase of RFU with increase in time till 20 min which indicated presence of enzymatic active rLC-TD/A protein. U represents 25 kDa un-cleaved SNAP-25 band and C represents 24 kDa cleaved band of SNAP-25. All the measurements were carried out in triplicate and mean data are presented along with the standard deviation

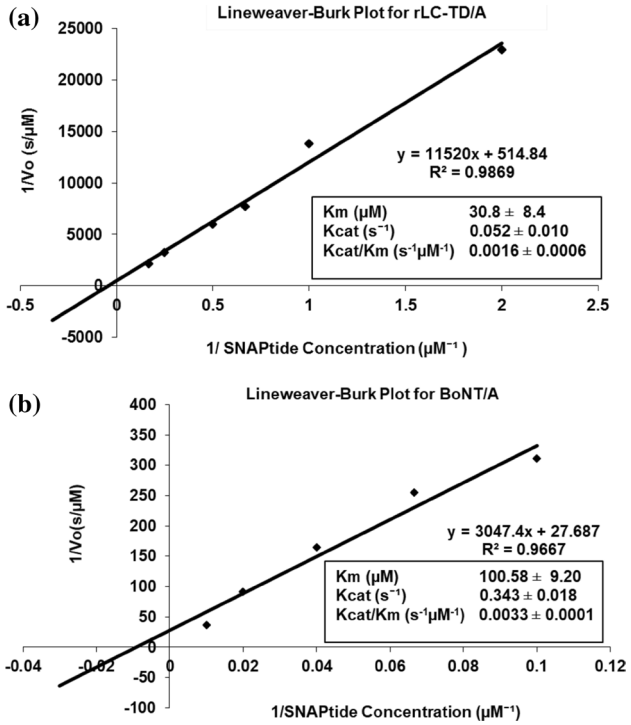

Fig. 7 Lineweaver–Burk plot and kinetic parameters for rLC-TD/A and BoNT/A kinetics. **a** Representative Lineweaver–Burk plot for LC-TD/A. **b** Lineweaver–Burk plot for BoNT/A. The plot shows the trendline for a single run. The kinetic parameters were calculated from Lineweaver–Burk plot of three individual runs

high to low pH. The addition of trypsin to the liposomes at pH 7.2 and 4.5 showed 3.28 ± 0.10 and 3.48 ± 0.25% K^+ release from vesicles, respectively, at 5 min time point. The lower K^+ release, equivalent to the basal release, in the presence of trypsin was indicative of the specificity of the vesicles to membrane proteins. rLC-TD/A showed 10.0 ± 0.5, 18.0 ± 1.0, 21.2 ± 2.6, and 23.5 ± 1.9% K^+ release after 1, 5, 10, and 15 min of protein addition to the liposomes, respectively (Fig. 8).

3.5 Far-UV Spectra of *rLC-TD/A*

Secondary structure of the globular proteins can be probed by far-UV spectra measurement [24, 28]. The far-UV spectra for rLC-TD/A displayed an alpha-helical protein pattern at pH 7.2, with a double minima structure at 208 and 222 nm, respectively (Fig. 9). The Mean Residue Weight Ellipticity at 208 and 222 nm was found to be 19982.26 ± 189.10 and 14246.35 ± 110.92 deg cm^2/dmol, respectively. The alpha-helical content was estimated to be 56.0%, beta-strand as 18.3% and others (random coil and turns) as 25.7%.

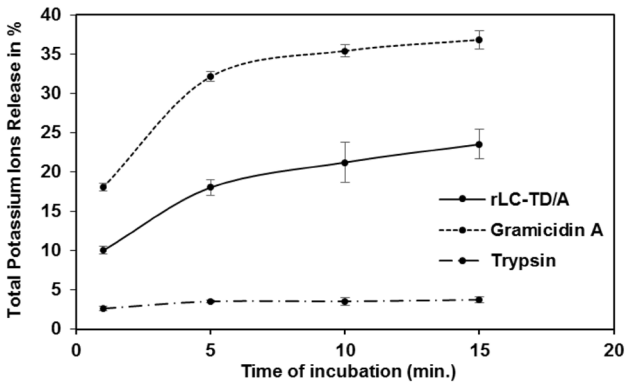

Fig. 8 Time dependent % potassium release due to channel formation by rLC-TD/A in *trans*-compartmental pH System. Gramicidin A and trypsin are included as positive and negative control, respectively. The data presented here is expressed as means ± standard deviation (n = 3)

4 Discussion

The translocation variants of BoNT are vital for understanding of the translocation process as the molecular architecture involved in the process is not well understood. The translocation domain of the BoNT is required for the

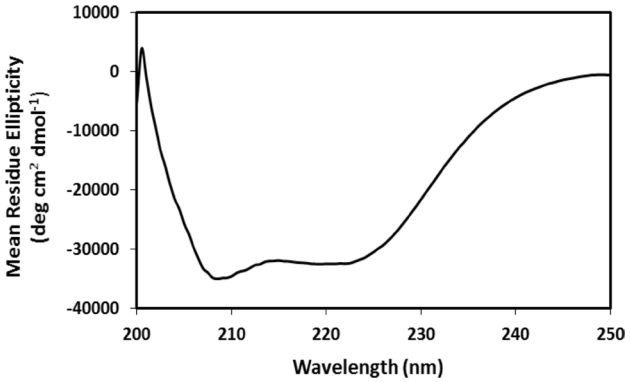

Fig. 9 Far-UV spectra of rLC-TD/A dissolved in 20 mM Tris–HCl buffer, pH 7.4, containing 300 mM NaCl at 25 °C. The recorded scan is the average of three scans

translocation of the catalytic domain across the endosomal or synaptic vesicle membranes. The rLC-TD/A domain of BoNT/A can be used for the study of the translocation mechanism involved in the intoxication process, with only low levels of toxicity. The expression of LC [29], and TD [30] domains in *E. coli* expression systems have been reported before. The classical purification method for the production of LC-TD/A involves the use of whole length toxin, trypsinization, and chromatographic techniques [14]. The production of such constructs is a challenging process owing to the toxicity of BoNT, as this method is a long and laborious process involving biosafety concerns as well as possibility of cross contamination of RBD region during the purification process. The expression and purification involving toxin handling can be avoided by using recombinant LC-TD/A construct. The cloning and expression methods, reported previously for rLC-TD/A, involves majorly two methods: (1) amplification of region of interest from clostridial DNA sequence [15, 16] and (2) ligation of LC and TD DNA obtained from two separate vectors [13]. However, both methods involve the use of C. botulinum culture which require regulatory issues, including a facility to address biosafety concerns. As an alternative approach, we have utilized a PCR amplified DNA fragment encoding LC-TD/A region from the DrBoNT/A clone, which is a non-toxic variant of BoNT/A, previously produced in our lab [17]. The method described in the current paper involves use of heterologous expression *E. coli* system for production of rLC-TD/A protein which resulted in 2 to 20-fold higher yield (1.5 mg per g cell paste or 1.5 mg per l of *E. coli* culture) with > 95% purity as compared to the methods published (20 fold higher than that reported by [15], and twofold higher than that by [16], respectively). The major benefit of our method includes non-requirement of biosafety level regulations which makes it an economical purification procedure. The rLC-TD/A produced by our method is also free of neurotoxin or RBD contamination and therefore it will be less toxic than BoNT/A. The purified protein can also be used for crystallization purposes. Also, the rLC-TD/A protein produced is of high concentration (~0.8 mg/ml) which will be apt for structure studies conducted using far-UV and near-UV circular dichroism spectroscopy.

We have constructed a 7.8 kb pEt-45b (+) expression cassette, including 5.15 kb synthetic DNA encoding *E. coli* codon bias, and a 2.65 kb fragment encoding rLC-TD/A gene (Fig. 3). The DNA and amino acid sequencing revealed the ORF encoding 871 amino acids corresponding to LC-TD/A sequence of BoNT/A. We successfully designed and cloned the rLC-TD/A construct which could express rLC-TD/A. We also demonstrated the purification of rLC-TD/A by using a combination of affinity chromatography, trypsinization and anion-exchange chromatography. The cobalt column elutes showed the major impurity band at ~74 kDa along with the rLC-TD/A band (Fig. 4). The literature search on *E. coli* expressed proteins showed that ~74 kDa protein is known as formyl transferase or YfbG protein which has a pI of 6.3 [31]. The primary sequence of this protein showed the presence of 4.1% histidine residue clusters and various trypsinization sites (P77398, SwissProt Access Code). Therefore, the second step of purification procedure that is trypsinization resulted in solving three major issues: (1) the removal of ~74 kDa band, (2) nicking of rLC-TD/A protein required for its activation and (3) removal of misfolded/poorly folded protein. The final purification step involving use of QAE-A-50 anion-exchange column resulted in rLC-TD/A of > 95% purity (Fig. 4). Furthermore, the western blot results confirmed the identity of protein (Fig. 5).

Additionally, the purified rLC-TD/A protein was a functionally active protein (Fig. 6). The cell-based SNAP-25 assay showed that the rLC-TD/A protein is ~18% less active than the whole toxin (Fig. 6b). To test the translocation capability and verify that the purified rLC-TD/A translocate to the cytosol in a similar way as toxin does, we use an endosomal acidification inhibitor, bafilomycin. Bafilomycin is known inhibitor of proton pumps in endosomes [31, 32]. The cells pre-incubated with 2 μM bafilomycin and later with rLC-TD/A did not show SNAP-25 cleavage indicating that the rLC-TD/A translocates to cytosol through acidified endosomes similar to BoNT/A toxin. The SNAP-25 cleavage assay results indicate that rLC-TD/A protein possesses the ability to enter the cells via an endocytic pathway causing subsequent substrate cleavage in the cytosol. The high concentration of rLC-TD/A protein was used for cell assay because of the absence of C-terminal receptor binding domain, which increases the efficiency of internalization process of rLC-TD/A [13]. Notably, the cell-based assay result was comparable with the earlier reported translocation activity of rLC-TD/A protein in the Neuro-2a cells [13]. The

results indicated the purified rLC-TD/A is a catalytic active translocation construct as demonstrated by both in vitro (SNAPtide®) and cell-based activity assays.

We have also estimated enzyme kinetic parameters for rLC-TD/A which has not been reported before. The kinetic parameters will be useful for the study of molecular mechanism when compared with rLC/A and BoNT/A. The calculated kinetic parameters of rLC-TD/A (Fig. 7a) was compared with that of rLC/A (earlier published by our group, [22]) and BoNT/A, with experiments performed under similar conditions. The results showed 2.8-fold increase in K_m of rLC-TD/A compared to the rLC/A (Table 2). The higher K_m value indicated a lower accessibility of SNAPtide 521® to the active site in rLC-TD/A as compared to rLC/A, which also leads to an overall decrease in catalytic efficiency of the enzyme. The K_m for BoNT/A was found to be threefold higher than rLC-TD/A (Fig. 7b). Overall, the K_m values indicated that the rLC/A has a higher apparent affinity for smaller substrate than rLC-TD/A, and rLC-TD/A has higher apparent affinity than the whole toxin, BoNT/A. The order of increasing apparent affinity for the peptide substrate would be as follows: rLC/A > rLC-TD/A > BoNT/A. The data suggest that the absence of HC makes the active site more accessible to the substrate. This observation is consistent with the report that N-terminal of the HC belt region occludes the enzyme active site [3, 32]. The purified rLC-TD/A and BoNT/A both contain the belt region and their K_m values are substantially higher reflecting the occlusion of the active site. Furthermore, K_{cat}/K_m ratio corresponding to the catalytic efficiency of rLC-TD/A was found to be about 8.1-fold less than that of rLC/A. However, K_{cat}/K_m of BoNT/A is 2.1-fold higher than rLC-TD/A (Table 2). Higher catalytic efficiency means faster product release and higher turnover. This would indicate that even though the active site accessibility in rLC-TD/A and BoNT/A is different the TD domain sufficiently represents the BoNT/A for the effect of the HC on the enzymatic activity of the LC domain. The reason for using different substrate is primarily due to historical sequence of experiments; however, these were within appropriate substrate and enzyme concentration range for enzyme kinetics (at least 10-fold difference in enzyme and substrate concentrations). Additionally, the substrate used for BoNT/A and LC/A differ in the FRET system, which could potentially affect the fluorescence efficiency, as reported by the manufacturer [33, 34]. Therefore, this explanation needs further verification with full-length substrate. For the purpose of work described in this report, the value of our observations is that rLC-TD/A, rLC/A, and BoNT/A exhibit kinetic parameters within the range of reported values [35], and rLC-TD/A will become a useful system for further studies.

Table 2 Enzyme kinetic parameters of rLC-TD/A, BoNT/A, and rLC/A

Kinetics parameters	rLC/A*	rLC-TD/A	BoNT/A
K_m (μM)	11.1 ± 0.86	30.8 ± 8.4	100.58 ± 9.20
K_{cat} (s^{-1})	0.15 ± 0.01	0.052 ± 0.010	0.343 ± 0.018
K_{cat}/K_m (s^{-1} μM^{-1})	0.013 ± 0.001	0.0016 ± 0.0006	0.0033 ± 0.0001

The kinetic parameters were calculated from the Lineweaver–Burk plot of each of the triplicate runs. The mean data are presented along with the standard deviation

*From Feltrup and Singh [22]

We have also substantiated the translocation capability of purified rLC-TD/A construct as it could be potentially utilized in channel conducting translocation studies. The channel assay performed using K^+ loaded liposomes in a *trans*-compartmental pH System showed the increase in release of K^+ with the transient increase of time up to 15 min after incubation with rLC-TD/A protein (Fig. 8). The assay results demonstrated the capability of purified rLC-TD/A for transport studies, similar to published reports [7]. The secondary structure determination using far-UV spectra confirmed the presence of majorly alpha-helical and proper folded rLC-TD/A protein (Fig. 9). Our results demonstrated that the purified rLC-TD/A protein is well folded with functionally active states including the belt region.

A few major issues with BoNT mechanism that is still not settled are translocation molecular structure and mechanism, the existence of oligomer, and how the disulfide bonds are reduced in the cells. The rLC-TD/A construct purified in the present study could be employed to address these unknown/debatable questions because it is not as toxic as BoNT, and therefore it could be used in high concentrations for mechanism oriented studies. The rLC-TD/A constructs have also been used earlier in the channel activity studies involving voltage gated lipid bilayer systems [4, 35]. Hence, such recombinant constructs can be used for translocation activity assays in labs without the requirement of biosafety regulations. Use of non-toxic fragments of BoNT typically C-terminal of HC as an immunogen or as recombinant vaccines for BoNT has been reported before [36–38]. The potential use of rLC-TD/A as an immunogen has also been demonstrated in published work by Chaddock et al [15]. To sum up, the rLC-TD/A construct could prove to be a useful tool in either mechanism driven research or in biomedical application.

5 Conclusions

The development of rLC-TD/A constructs is advantageous not only for the advancement of research related to translocation mechanism but it also eliminates the use of

Clostridium botulinum culture for purification of these subunits which requires high biosafety regulations. We have successfully demonstrated the purification of >95% pure and soluble rLC-TD/A with a yield of 1.50 ± 0.35 mg protein per g cell paste using the three step purification process, without need to use detergent in any step of purification. The purified protein is functionally active and well-folded. The purified rLC-TD/A protein can serve as useful tools for ion-channel studies, translocation studies, pH-sensing studies, protein-membrane interactions and protein–protein interactions. Information from these studies will help scientists to understand various aspects of biochemistry, which will ultimately help in designing better countermeasures for botulinum neurotoxin.

Acknowledgements This work was supported in part by a grant from the National Institute of Allergy and Infectious Diseases (NIAID—1U01A1078070-02) and by Maryada Foundation. The authors would like to thank Mr. Stephen J. Riding for his assistance in purification procedures. The authors also thank Dr. Gowri Chellappan for her assistance in liposome preparation procedures.

Author Contributions Conceived the idea: NT, HD, BS. Designed and carried out the experiments: HD, NT, RK. Kinetics experiments: KP, GA. Analyzed the data: HD, RK, BS. Contributed reagents/materials/analysis tools: SC, BS. Offered comments on data interpretation and manuscript preparation: SC, RK, BS. Wrote the manuscript: HD, BS.

Compliance with Ethical Standards

Conflict of interest The authors declare no conflict of interest.

References

1. Singh BR (2000) Intimate details of the most poisonous poison. Nat Struct Mol Biol 7:617–619
2. Schiavo G, Matteoli M, Montecucco C (2000) Neurotoxins affecting neuroexocytosis. Physiol Rev 80:717–766
3. Lacy DB, Tepp W, Cohen AC et al (1998) Crystal structure of botulinum neurotoxin type A and implications for toxicity. Nat Struct Biol 5:898–902. doi:10.1038/2338
4. Montal M (2010) Botulinum neurotoxin: a marvel of protein design. Annu Rev Biochem 79:591–617. doi:10.1146/annurev.biochem.051908.125345
5. Fischer A, Sambashivan S, Brunger AT, Montal M (2012) Beltless translocation domain of botulinum neurotoxin A embodies a minimum ion-conductive channel. J Biol Chem 287:1657–1661. doi:10.1074/jbc.C111.319400
6. Blaustein RO, Germann WJ, Finkelstein A, DasGupta BR (1987) The N-terminal half of the heavy chain of botulinum type A neurotoxin forms channels in planar phospholipid bilayers. FEBS Lett 226:115–120
7. Shone CC, Hambleton P, Melling J (1987) A 50-kDa fragment from the NH2-terminus of the heavy subunit of *Clostridium botulinum* type A neurotoxin forms channels in lipid vesicles. Eur J Biochem 167:175–180
8. Binz T, Rummel A (2009) Cell entry strategy of clostridial neurotoxins. J Neurochem 109:1584–1595. doi:10.1111/j.1471-4159.2009.06093.x
9. Montecucco C, Molgo J (2005) Botulinal neurotoxins: revival of an old killer. Curr Opin Pharmacol 5:274–279. doi:10.1016/j.coph.2004.12.006
10. Koriazova LK, Montal M (2003) Translocation of botulinum neurotoxin light chain protease through the heavy chain channel. Nat Struct Biol 10:13–18. doi:10.1038/nsb879
11. Fischer A, Montal M (2007) Crucial role of the disulfide bridge between botulinum neurotoxin light and heavy chains in protease translocation across membranes. J Biol Chem 282:29604–29611. doi:10.1074/jbc.M703619200
12. Fischer A, Montal M (2007) Single molecule detection of intermediates during botulinum neurotoxin translocation across membranes. Proc Natl Acad Sci USA 104:10447–10452. doi:10.1073/pnas.0700046104
13. Fischer A, Mushrush DJ, Lacy DB, Montal M (2008) Botulinum neurotoxin devoid of receptor binding domain translocates active protease. PLoS Pathog 4:e1000245. doi:10.1371/journal.ppat.1000245
14. Sathyamoorthy V, Dasgupta BR, Foley J, Niece RL (1988) Botulinum neurotoxin type A: cleavage of the heavy chain into two halves and their partial sequences. Arch Biochem Biophys 266:142–151
15. Chaddock JA, Herbert MH, Ling RJ et al (2002) Expression and purification of catalytically active, non-toxic endopeptidase derivatives of *Clostridium botulinum* toxin type A. Protein Expr Purif 25:219–228
16. Jensen MJ, Smith TJ, Ahmed SA, Smith LA (2003) Expression, purification, and efficacy of the type A botulinum neurotoxin catalytic domain fused to two translocation domain variants. Toxicon 41:691–701. doi:10.1016/S0041-0101(03)00042-4
17. Yang W, Lindo P, Riding S, Chang T, Cai S, Van T, Kukreja R, Zhou Y, Vasa K, Singh BR (2008) Expression, purification and comparative characterisation of enzymatically deactivated recombinant botulinum neurotoxin type A. Botulinum J 1:219. doi:10.1504/TBJ.2008.026477
18. Baskaran P, Lehmann TE, Topchiy E et al (2013) Effects of enzymatically inactive recombinant botulinum neurotoxin type A at the mouse neuromuscular junctions. Toxicon 72:71–80. doi:10.1016/j.toxicon.2013.06.014
19. Meyers JA, Sanchez D, Elwell LP, Falkow S (1976) Simple agarose gel electrophoretic method for the identification and characterization of plasmid deoxyribonucleic acid. J Bacteriol 127:1529–1537
20. Laemmli UK (1970) Cleavage of structural proteins during the assembly of the head of bacteriophage T4. Nature 227:680–685
21. Towbin H, Staehelin T, Gordon J (1979) Electrophoretic transfer of proteins from polyacrylamide gels to nitrocellulose sheets: procedure and some applications. Proc Natl Acad Sci USA 76:4350–4354
22. Feltrup TM, Singh BR (2012) Development of a fluorescence internal quenching correction factor to correct botulinum neurotoxin type A endopeptidase kinetics using SNAPtide. Anal Chem 84:10549–10553. doi:10.1021/ac302997n
23. Rasetti-Escargueil C, Machado CB, Preneta-Blanc R et al (2011) Enhanced sensitivity to Botulinum type A neurotoxin of human neuroblastoma SH-SY5Y cells after differentiation into mature neuronal cells. Botulinum J 2:30–48. doi:10.1504/TBJ.2011.041814
24. Chellappan G, Kumar R, Santos E et al (2015) Structural and functional analysis of botulinum neurotoxin subunits for pH-dependent membrane channel formation and translocation. Biochim Biophys Acta 1854:1510–1516. doi:10.1016/j.bbapap.2015.05.013
25. Mayer LD, Bally MB, Hope MJ, Cullis PR (1986) Techniques for encapsulating bioactive agents into liposomes. Chem Phys Lipids 40:333–345

26. Cai S, Singh BR (2001) Role of the disulfide cleavage induced molten globule state of type a botulinum neurotoxin in its endopeptidase activity. BioChemistry 40:15327–15333
27. Louis-Jeune C, Andrade M, Perez-Iratxeta C (2012) Prediction of protein secondary structure from circular dichroism using theoretically derived spectra. Proteins 80(2):374–381. doi:10.1002/prot.23188
28. Kumar R, Kukreja RV, Cai S, Singh BR (2014) Differential role of molten globule and protein folding in distinguishing unique features of botulinum neurotoxin. Biochim Biophys Acta 1844:1145–1152. doi:10.1016/j.bbapap.2014.02.012
29. Li L, Singh BR (1999) High-level expression, purification, and characterization of recombinant type A botulinum neurotoxin light chain. Protein Expr Purif 17:339–344. doi: 10.1006/prep.1999.1138
30. Lacy DB, Stevens RC (1997) Recombinant expression and purification of the botulinum neurotoxin type A translocation domain. Protein Expr Purif 11:195–200. doi: 10.1006/prep.1997.0772
31. Bolanos-Garcia VM, Davies OR (2006) Structural analysis and classification of native proteins from *E. coli* commonly co-purified by immobilised metal affinity chromatography. Biochim Biophys Acta 1760:1304–1313. doi:10.1016/j.bbagen.2006.03.027
32. Brunger AT, Breidenbach MA, Jin R et al (2007) Botulinum neurotoxin heavy chain belt as an intramolecular chaperone for the light chain. PLoS Pathog 3:1191–1194. doi:10.1371/journal.ppat.0030113
33. Todd C, Shine N et al (2005) Comparison of activity of botulinum neurotoxin type a holotoxin and light chain using SNAPtide® FRET substrates. In: 5th International conference on basic and therapeutic aspects of botulinum and tetanus toxins, List Labs Poster, Denver, CO. https://www.listlabs.com/mediafiles/posters/BTA-LcA-comparison-poster-4.pdf
34. Todd C, Shine N, Crawford K (2008) New high affinity antibodies against botulinum neurotoxin type A. In: 6th Annual ASM biodefense and emerging diseases research meeting, List Labs Poster, Baltimore, MD. https://www.listlabs.com/mediafiles/posters/Biodefense-poster--022108-8.pdf
35. Fischer A (2013) Synchronized chaperone function of botulinum neurotoxin domains mediates light chain translocation into neurons. Curr Top Microbiol Immunol 364:115–137. doi:10.1007/978-3-642-33570-9_6
36. Smith LSH (1988) Botulism: the organism, its toxins, the disease, 2nd edn. Charles C Thomas Publisher, Limited, Springfield
37. Clayton MA, Clayton JM, Brown DR, Middlebrook JL (1995) Protective vaccination with a recombinant fragment of *Clostridium botulinum* neurotoxin serotype A expressed from a synthetic gene in *Escherichia coli*. Infect Immun 63:2738–2742
38. Byrne MP, Smith LA (2000) Development of vaccines for prevention of botulism. Biochimie 82:955–966